Chapter 1

Introduction

Introduction

World production of farmed shrimps has been dominated by *Penaeus monodon* and *Litopenaeus vannamei*. In Southeast Asian, shrimp aquaculture has rapidly increased and developed economic importance over several decades, and Thailand being the main shrimp farming country in the region. In practice, an insufficient supply of postlarvae and disease bursts in *P. monodon* culture have prompted more shrimp farmers to seek alternative species, such as the banana shrimp, *Penaeus* (*Fenneropenaeus*) *merguiensis*. *P. merguiensis* is a white shrimp that has attracted attention and has prospects as a farmed species (Sangpradab *et al*., 1987; Chandumpai, 1998). This species can reach full ovarian maturation in captivity and spawn naturally, without eyestalk ablation. Thus, hatchery production is reliable and independent from the wild stocks. This would allow a greater chance of domestication, and selective breeding programs for fast growth and/or disease resistance can be performed. Banana shrimp requires lower dietary protein, can be cultured at high density and they can live in estuaries. Reproduction can be controlled using a combination of environmental and nutritional manipulation. Banana shrimp can be accommodated in small maturation systems. Larval rearing appears to be easier than for *P. monodon*. (Zacharia and Kakati, 2002; Tung, 2001).

Most hatcheries use hatch rates as a key performance indicator of broodstock. However, hatch rate is influenced by several factors. Male performance is dependent on sperm quantity per spermatophore and fertilisation capability of the sperm, while female performance is dependent on such parameters as total eggs spawned per spawning, egg quality, and hatchability. During egg formation in the female, vitellogenesis, all of the nutritional and other requirements for successful hatching are packaged in the egg at this time. In penaeid shrimps, there are no functional mouthparts until the nauplius stage, and in fact the larvae do not actually become self-feeding until the zoea stage. Therefore, the larvae are totally dependent on accumulated yolk,

vitellin (major eggs yolk proteins) for nutrition during the first 36 to 48 hours after hatching. All of the nutritional and other compounds necessary for successful embryogenesis and early larval development must have all been previously stored during egg maturation within the mother. The yolk and its associated compounds are a major determinant of egg quality. During vitellogenesis, vitellogenin is synthesized intra- or extra-ovary and then transported via hemolymph to the developing oocytes, where it subsequently forms vitellin, which is accumulated in oocytes causing a significant increase in their diameter (Meusy and Charniax-Cotton, 1984; Charniax-Cotton, 1985). In order to enable selection of suitable female spawners for stable seed production or inducible maturation without eyestalk ablation, it is necessary to understand the mechanism of ovarian maturation, including studies elucidating yolk protein sequence and structure, sites of vitellogenesis, dynamics of vitellogenin mRNA expression and vitellogenin processing in banana shrimp.

The site of vitellogenin synthesis varies according to species. Among oviparous animals, vitellogenin is synthesized by liver in nonmammalian vertebrates, fat body in insects and intestine in nematodes, whereas in crustaceans the site of vitellogenesis is still controversial. Recently, the source of yolk proteins and changes in vitellogenin mRNA expression in crustacean has been investigated. Hepatopancreas was found to be a site of vitellogenin synthesis in *Macrobrachium rosenbergii* (Jayasankar *et al*., 2002), *Pandalus hypsinotus* (Tsutsui *et al*., 2004) and *Charybdis feriatus* (Mak *et al*., 2005) whereas in *Penaeus semisulcatus* (Avarre *et al*., 2003), *P. monodon* (Tiu *et al*., 2006), *Marsupenaeus japonicus* (Tsutsui *et al*., 2000; Tsutsui *et al*., 2005) and *L. vannamei* (Raviv *et al*., 2006), ovary and hepatopancreas are found to be sites of Vg synthesis. Currently, full-length vitellogenin cDNA has been determined in only 11 species of decapod crustacean, including *P. merguiensis*.

The isolation, purification, characterization of purified vitellogenin and vitellin to generate specific anti-vitellin antibodies, used for determining Vg in hemolymph at various stages of ovarian development in banana shrimps by enzyme linked immunosorbent assay (ELISA) are published in the PhD thesis of Jongruk Auttarat (2005). The present work is concerned with extending the knowledge about vitellogenesis in this shrimp by characterizing purified vitellin in more detail such as determining the N-terminal amino acid sequence, amino acid composition, pI value and protease activity. Moreover, this work also determined the sites of

vitellogenin synthesis, the full-length vitellogenin cDNA in ovary, a partial vitellogenin cDNA sequence at 3' end from hepatopancreas, the dynamics of vitellogenin mRNA at various stages of ovarian development in intact mature female shrimps and several bioinformatics tools were used to perform analyses such as sequences comparison, nucleotide-amino acid different analysis, phylogenetic tree analysis and prediction of tertiary structure.

Information is limited about alterations in the molecular composition of the egg in *P. merguiensis* and other decapod crustaceans, reflecting changes in gene and protein activities during ovarian development. Therefore, proteomic analysis might be a powerful tool for investigating the nature protein changes during ovarian development. High-resolution two-dimensional polyacrylamide gel electrophoresis (2-D PAGE) has been used in this study. Differences in protein expression during embryo development have been studied in fruit fly (Sakoyama and Okubo, 1981; Trumbly and Jarry, 1983). We have established the first 2-D map of various GSI values of ovarian development in banana shrimp including GSI 0.995 ± 0.104, 2.998 ± 0.175 and 8.273 ± 0.092. Electrophoretic patterns were compared and identified by tryptic digestion, followed by mass spectrometry and analysis by a combination of Mascot and ProteinLynx Software searches. Since only a few proteins have been sequenced from shrimp, protein identification must rely on cross-species matches to sequences from other species, such as the fruit fly *Drosophila melanogater*, California spiny lobster *Panulirus interruptus* and so on. This study presents the analysis of eighty-one identified protein spots, and in order to identify proteins other than vitellin, importance during ovarian development in penaeids.

Review of Literatures

1. *Penaeus* (*Fenneropenaeus*) *merguiensis*

1.1 Economic importance and geographic distribution

Penaeus merguiensis or banana shrimp is one of the important species for fisheries and aquaculture in the Indo-West Pacific. The species ranges from the Persian Gulf and Pakistan through the Malay Archipelago and South China Sea to Australia, where it is found from Western Australia all the way around the north coast to northern New South Wales as shown in Fig. 1 (Holthuis, 1980). The total banana shrimp capture around the world reported to FAO for 2004 was 91,672 tons with aquaculture production of 83,185 tons (Fig. 2A and 2B) (Food and Agriculture Organization of the United Nations (FAO), 2006, available: http://www.fao.org/figis/servlet/species?fid=2583). The production from aquaculture of this species keeps increasing and it has become an important species for aquaculture since 2001. The countries with the largest total catches were Indonesia (65,230 tons) and Thailand (9,200 tons) as of 1999. An article in the December 2001 issue of World Aquaculture Society (WAS), 2006, available: http://www.was.org, reviewed banana shrimp and its prospects as a farmed species. This shrimp has several advantages: easy larval rearing, good survival in extensive and semi-intensive ponds, toleration of a wide range of salinities and temperature, minimal size variation, natural maturation and spawning in captivity, it can be grown at high densities and it is readily available in the wild, meaning that wild-caught breeders are cheaper than for *P. monodon*. However, banana shrimp also has some disadvantages such as a slow growth rate, limited information on biology and culture, rapid death at harvest and lack of species-specific commercial feeds.

Fig. 1 Species distribution of *Penaeus merguiensis*, banana shrimp, is shown as red areas.

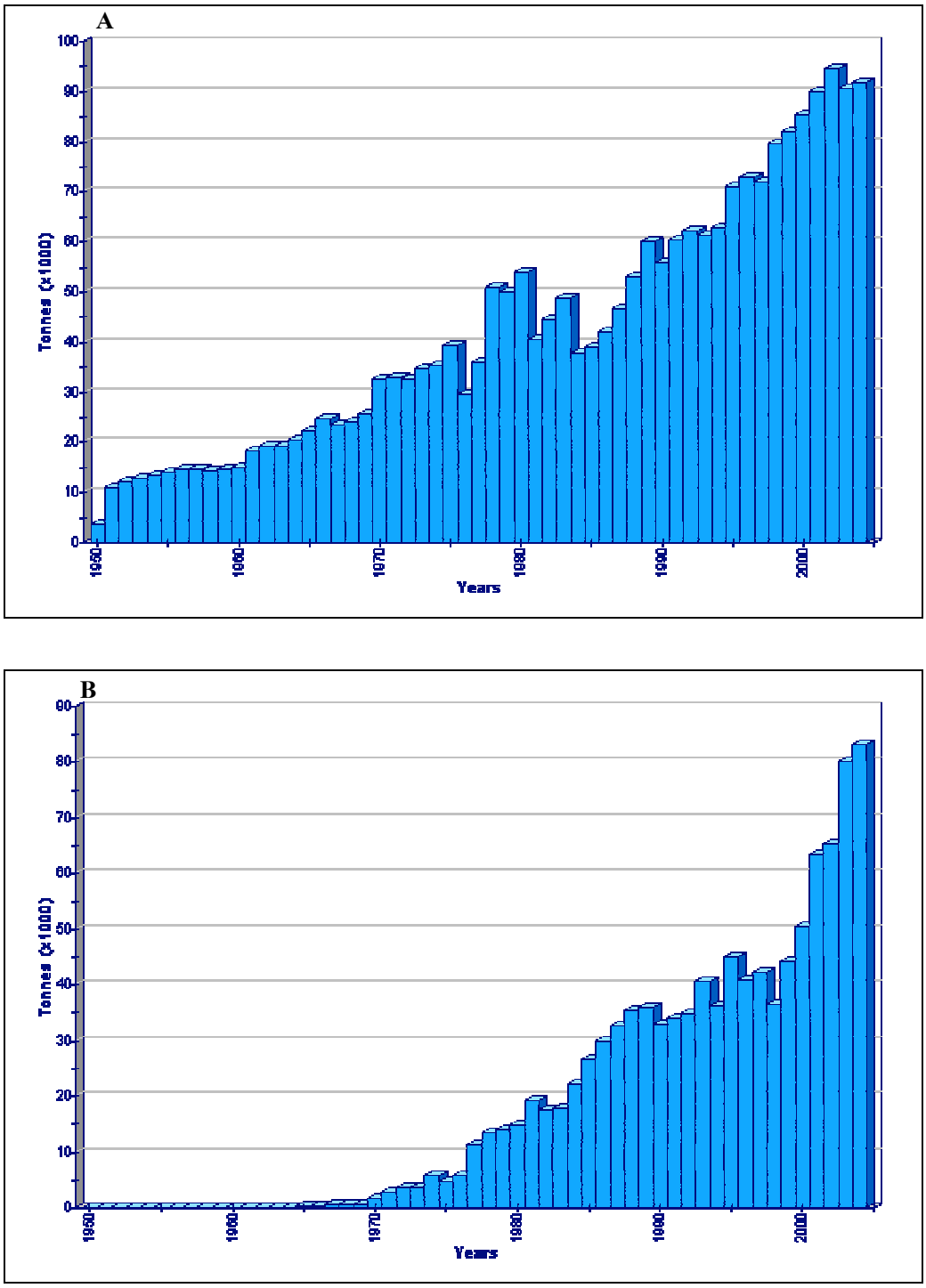

Fig. 2 Global wild capture production and global aquaculture production for *Penaeus merguiensis* is shown in Fig. 2A and 2B, respectively.

1.2 Banana shrimp taxonomy

P. merguiensis (Fig. 3) is member of the family Penaeidae. The penaeid shrimps belong to the largest phylum in the animal kingdom, the Arthropoda. This group of animals is characterised by the presence of paired appendages and a protective cuticle or exoskeleton that covers the whole animal. The subphylum Crustacea is predominantly aquatic species, that belong to 10 classes. Within the class Malacostraca, shrimp, together with crayfish, lobsters and crabs, belong to the order Decapoda as shown below. Many species in the old genus *Penaeus* have been reassigned, based on morphological differences, to new genera in the family Penaeidae: *Farfantepenaeus*, *Fenneropenaeus*, *Litopenaeus* and *Marsupenaeus* as shown in Table 1 (Perez-Farfante and Kensley, 1997).

Phylum-Arthropoda
Subphylum Crustacea
Class Malacostraca
Order Decapoda
Suborder Dendrobranchiata
Superfamily Penaeoidea
Family Penaeidae
Genus Penaeus
Subgenus Fenneropenaeus
Species merguiensis

Fig. 3 ***Penaeus merguiensis*** **or banana shrimp.**

Table 1 Old and new scientific names in genus *Penaeus*.

Old scientific name	New scientific name	Common name
Penaeus aztecus	*Farfantepenaeus aztecus*	Northern brown shrimp
Penaeus brasiliensis	*Farfantepenaeus brasiliensis*	Redspotted shrimp
Penaeus brevirostris	*Farfantepenaeus brevirostris*	Crystal shrimp, Pink shrimp
Penaeus chinensis	*Fenneropenaeus chinensis*	Chinese white shrimp
Penaeus duorarum	*Farfantepenaeus duorarum*	Northern pink shrimp
Penaeus esculentus	*Penaeus esculentus*	Brown tiger shrimp
Penaeus indicus	*Fenneropenaeus indicus*	Indian prawn
Penaeus japonicus	*Marsupenaeus japonicus*	Kuruma shrimp
Penaeus merguiensis	*Fenneropenaeus merguiensis*	Banana shrimp
Penaeus monodon	*Penaeus monodon*	Black tiger shrimp
Penaeus notialis	*Farfantepenaeus notialis*	Southern pink shrimp
Penaeus occidentalis	*Litopenaeus occidentalis*	Western white shrimp
Penaeus penicillatus	*Fenneropenaeus penicillatus*	Red tail prawn
Penaeus schmitti	*Litopenaeus schmitti*	Southern white shrimp
Penaeus semisulcatus	*Penaeus semisulcatus*	Green tiger shrimp
Penaeus setiferus	*Litopenaeus setiferus*	Northern white shrimp
Penaeus ensis	*Metapenaeus ensis*	Greasy back shrimp
Penaeus stylirostris	*Litopenaeus stylirostris*	Western blue shrimp, Blue shrimp
Penaeus subtilis	*Farfantepenaeus subtilis*	Southern brown shrimp
Penaeus vannamei	*Litopenaeus vannamei*	Pacific white shrimp

1.3 Penaeid shrimp morphology

The body of *P. merguiensis*, banana shrimp, is pale yellow or translucent and speckled with reddish brown dots. The exterior of penaeid shrimps is distinguished by a cephalothorax with a characteristic hard rostrum, and by a segmented abdomen (Fig. 4) (Primavera, 1990). Most organs, such as gills, digestive system and heart, are located in the cephalothorax, while the muscles are concentrated in the abdomen. In the head region, antennules and antennae perform sensory functions. In the thorax region, the maxillipeds are the first three pairs of appendages, modified for food handling, and the remaining five pairs are the walking legs (pereiopods). Five pairs of swimming legs (pleopods) are found on the abdomen (Bell and Lightner, 1988; Baily-Brock and Moss, 1992).

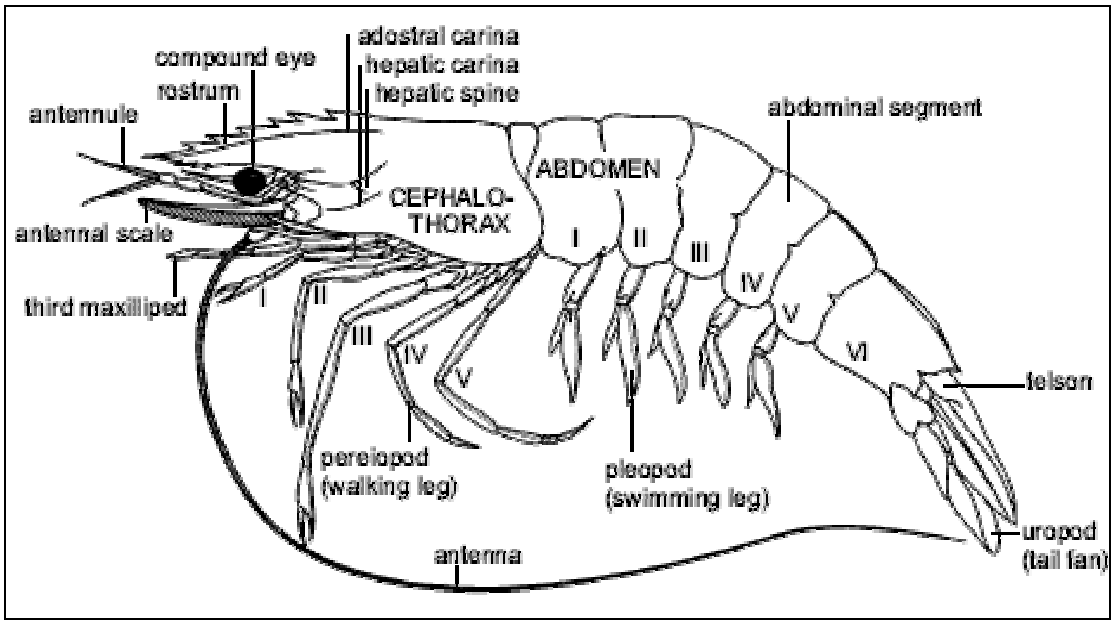

Fig. 4 Lateral view of the external morphology of penaeid.

The internal morphology of penaeid shrimp is showed in Fig. 5 (Primavera, 1990). Penaeids and other arthropods have an open circulatory system and, therefore, the blood and the blood cells are called hemolymph and hemocytes, respectively. Crustaceans have a muscular heart that is dorsally located in the cephalothorax. A large part of the cephalothorax in penaeid shrimp is occupied by the hepatopancreas. This digestive organ consists of diverticula of the intestine. Spaces between these hepatopancreatic tubules are hemolymph sinuses. The main functions of the hepatopancreas are the absorption of nutrients, storage of lipids and production of digestive enzymes (Johnson, 1980).

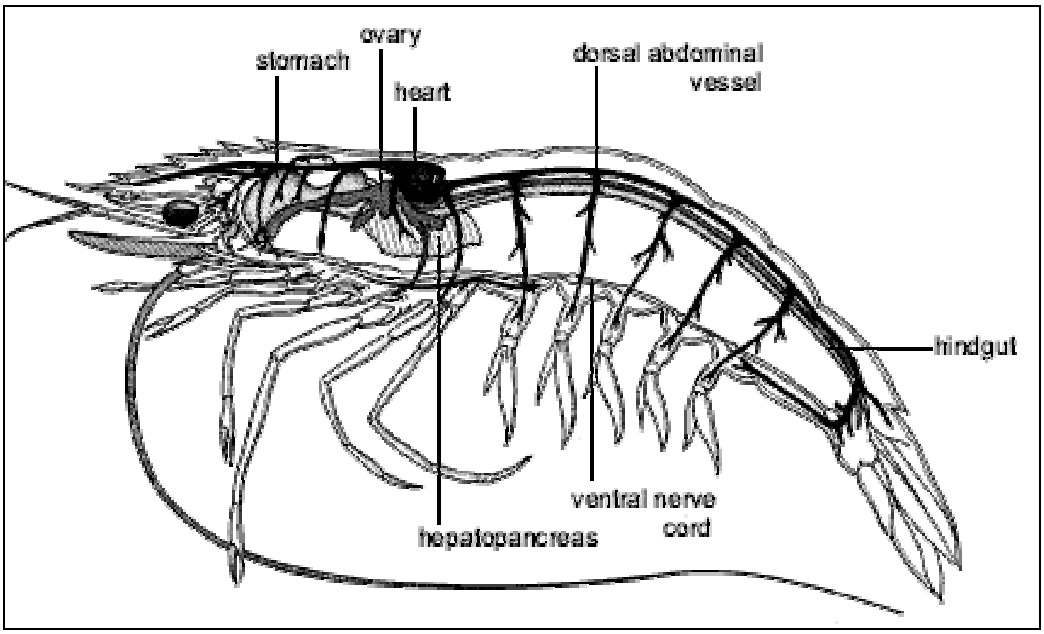

Fig. 5 Lateral view of the internal anatomy of a female penaeid.

The ovary lies dorsal to the gut and extends from the cephalothorax along the entire length of the tail (Fig. 6).

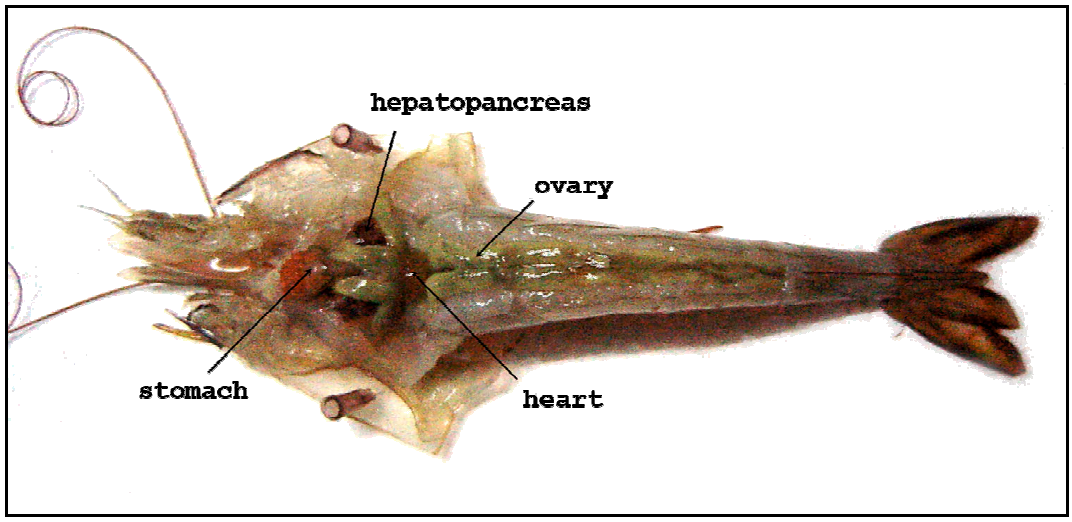

Fig. 6 The top view of the internal anatomy of a female *Penaeus merguiensis*.

1.4 Determination of ovarian development in penaeid shrimp by illuminating the internal body organs (hatchery technique) and other aspects of ovarian development

Ovarian maturation has been divided into stages that correspond with the external appearance of the ovaries, which can be estimated without microscopical sectioning (Dall *et al*., 1990). The determination of ovarian development by means of a bright underwater torch beam being passed along its side, only reveals the shadow of the ovary in the abdomen and is scored from 1 to 5 as shown in Fig. 7A (Australia Institute of Marine Science (AIMS), 2006, available: http://www.aims.gov.au/pages/research/mdef/mdef-00.html). The complete ovary extends from the head to the tail, and the majority of the ovary is found within the cephalothorax area. However, the intense pigmentation of the shell in this region prevents the visualisation of any ovarian outline as shown in Fig. 7B.

Stage 1 Immature, undeveloped ovary or previtellogenic stage; the ovary either does not cast any shadow or a thin opaque line is seen along the length of the tail. The ovary is translucent and unpigmented.

Stage 2 Developing ovary or early exogenous vitellogenic stage; the ovary can be visualised with a light beam as a large centrally located opaque rope-like structure.

Stage 3 Early mature, nearly ripe ovary or late exogenous vitellogenic stage; the ovary is visible through the exoskeleton and has light green color.

Stage 4 Mature or fully ripe ovary; the shadow cast by the ovary is large, resulting in a very distinct dark thick region extending the length of the abdomen, with an enlarged bulbous region directly behind the carapace, called the saddle. The wide saddle of ovarian tissue directly behind the carapace (stage 4) is indicative of an immediate pre-spawning female. A female scored as a stage 4 during the day is most likely to spawn that night. The light green color of ovary is changed into dark green color.

Stage 5 Spawning; the shrimp has already spawned. The ovary is translucent and unpigmented, similar to stage 1.

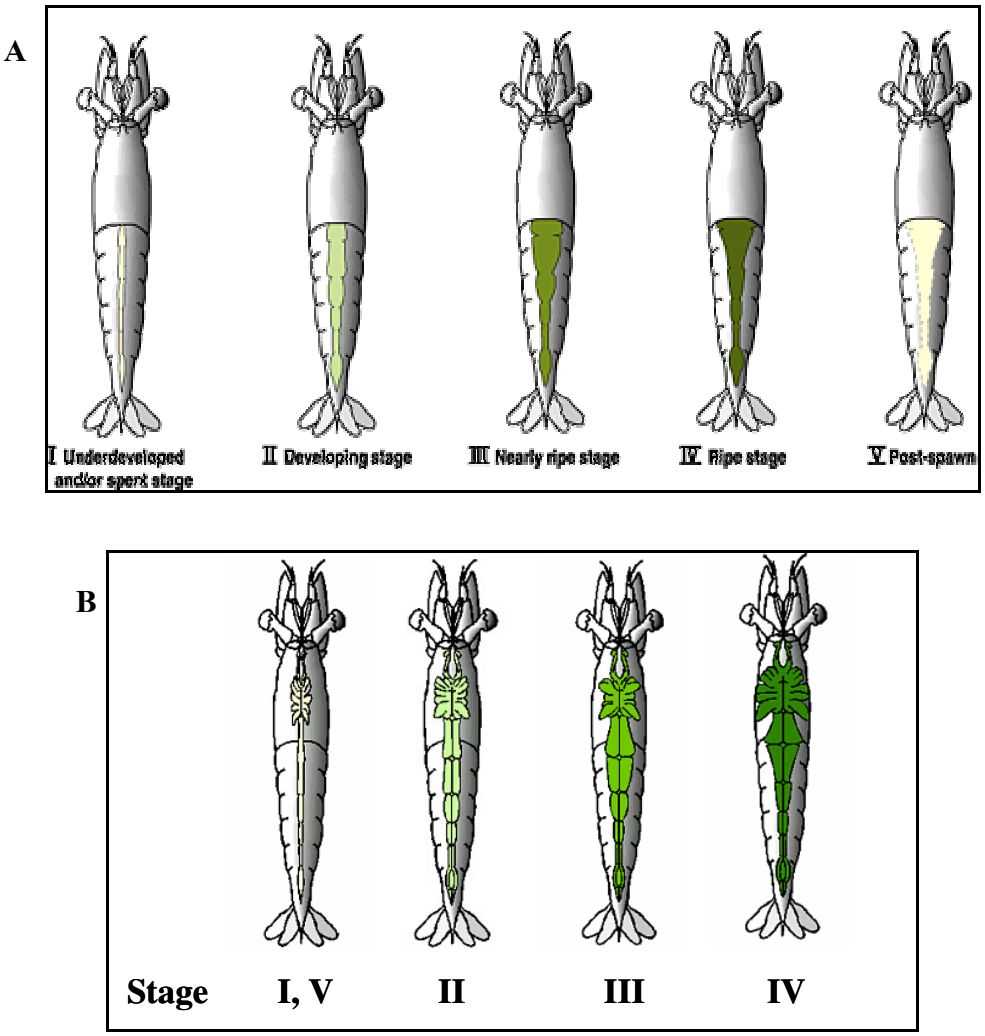

Fig. 7 The view observed by hatchery operators when female broodstock are graded for ovarian development by torchlight.

The view observed by torchlight (A) and the complete ovary extends from the head to the tail, the majority of the ovarian mass is within the cephalothorax region which cannot be observed by torchlight (B). (Australia Institute of Marine Science (AIMS), 2006, available: http://www.aims.gov.au/pages/research/mdef/mdef-00.html).

The relationship between gonadosomatic index (GSI), ovary color, oocyte development and ovarian development stages were determined by histological examination in *Aristaeomorpha foliacea* (Kao *et al*., 1999), *P. japonicus* (Yano, 1988), *P. monodon* (Peixoto *et al*., 2005), *Penaeus penicillatus*, *P. merguiensis*, *Metapenaeus affinis* and *Parapenaeopsis stylifera* (Ayub and Ahmed, 2002). Cross-sections of ovarian tissue in *P. stylifera* and physiological characterization in *P. merguiensis* at various stages of ovarian development are shown in Fig. 8 and Table 2, respectively (Ayub and Ahmed, 2002).

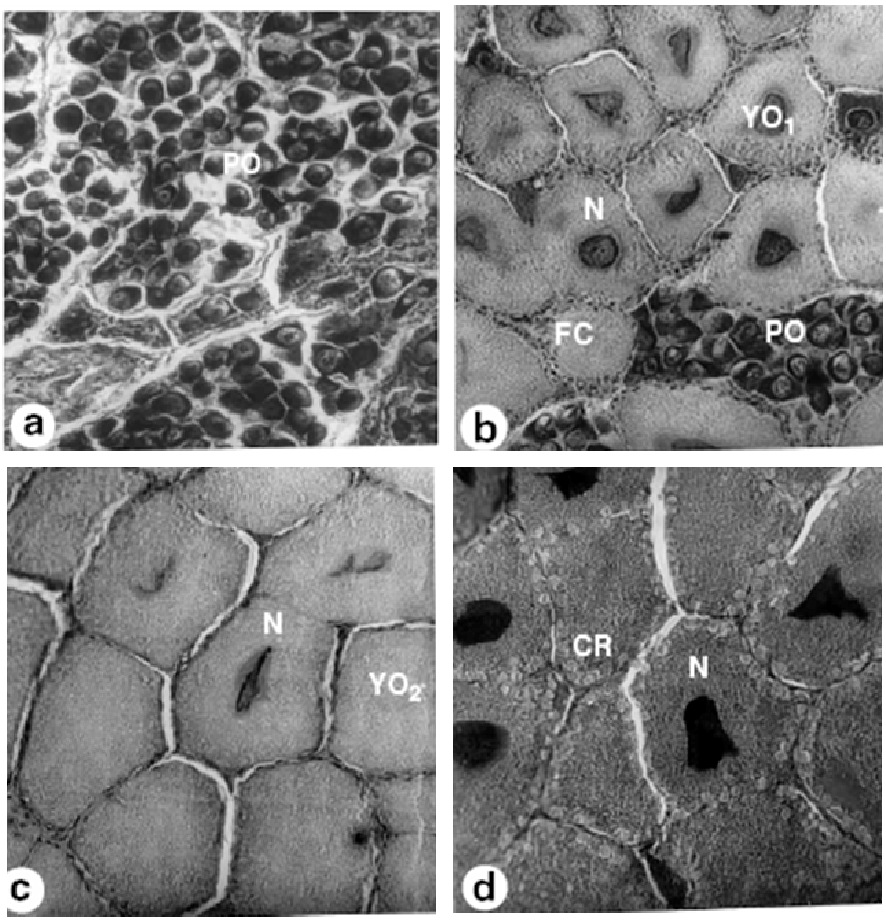

Fig. 8 Photomicrographs showing ovarian development.

(a) Section of an undeveloped ovary containing chromatin nucleolar and perinucleolar oocytes. (b) Developing ovary containing perinucleolar oocytes and yolkless oocytes. (c) Nearly ripe ovary showing yolky oocytes. (d) Fully ripe ovary showing oocytes with cortical bodies. PO, perinucleolar oocytes; YO_1, yolkless oocytes; YO_2, yolky oocytes; CR, oocytes with cortical bodies; FC, follicle cells; N, nucleus x 200 (Ayub and Ahmed, 2002).

Table 2 Characteristics of ovaries and oocyte physiology at various stages of ovarian development.

Stages	Frequency of types of oocytes	Color of ovary	Oocytes diameter (μm)
1 - undeveloped ovary	Predominance of perinucleolar oocytes. Chromatin nucleolar oocytes also present.	Translucent	32-65
2 – developing ovary	Perinucleolar oocytes occupy about 25% of the gonad. Yolkless oocytes abundant.	Translucent	75-125
3 – nearly ripe ovary	Perinucleolar oocytes present in small numbers. Yolky oocytes abundant.	White, cream, yellow green-yellow, green-white and light-green	100-200
4 – fully ripe ovary	Perinucleolar oocytes present in small numbers. Oocytes with cortical bodies abundant.	Green-yellow, green-white, light-green and dark-green	125-250

A high quality diet is necessary for the female to optimise egg quality. A major determinant of larval quality is the quality of yolk protein in the egg at the time of vitellogenesis, which will be described later, and the packaging of other critical molecules into the egg. The successful development of the embryo, hatching, and nauplius stages are dependent on egg quality. The larvae do not become self feeding until the protozoeae or zoeae stage, which is the first time that they become dependent on the quality of larval feeds rather than marternally-supplied nutrients.

An article from a manual for determination of egg fertility in *P. monodon* from the Australia Institute of Marine Science (AIMS), 2006, available: http://www.aims.gov.au describes that at stage 2 of ovarian development, inhibitory hormones in the eyestalk, arising from X-organ-sinus-gland neurosecretory complex, prevent further ovarian growth, especially if nutritional or environmental conditions are deemed unfavourable by the female. This will block further ovarian development.

A female can spawn several times within a single moult cycle. A new population of primary oogonia are recruited for each spawning event. If the female does spawn repeatedly within a moult cycle the same reserve of sperm within the thelycum, from the initial mating after moult, is used to fertilise the eggs. If the female does not spawn within a moult cycle the developed ovarian mass is reabsorbed a day or two before the next moult. After each moult the ovary is fully regressed and the ovary must mature anew. Fig. 9 shows the penaeid shrimp reproductive and moult cycle (Crocos and Kerr, 1983).

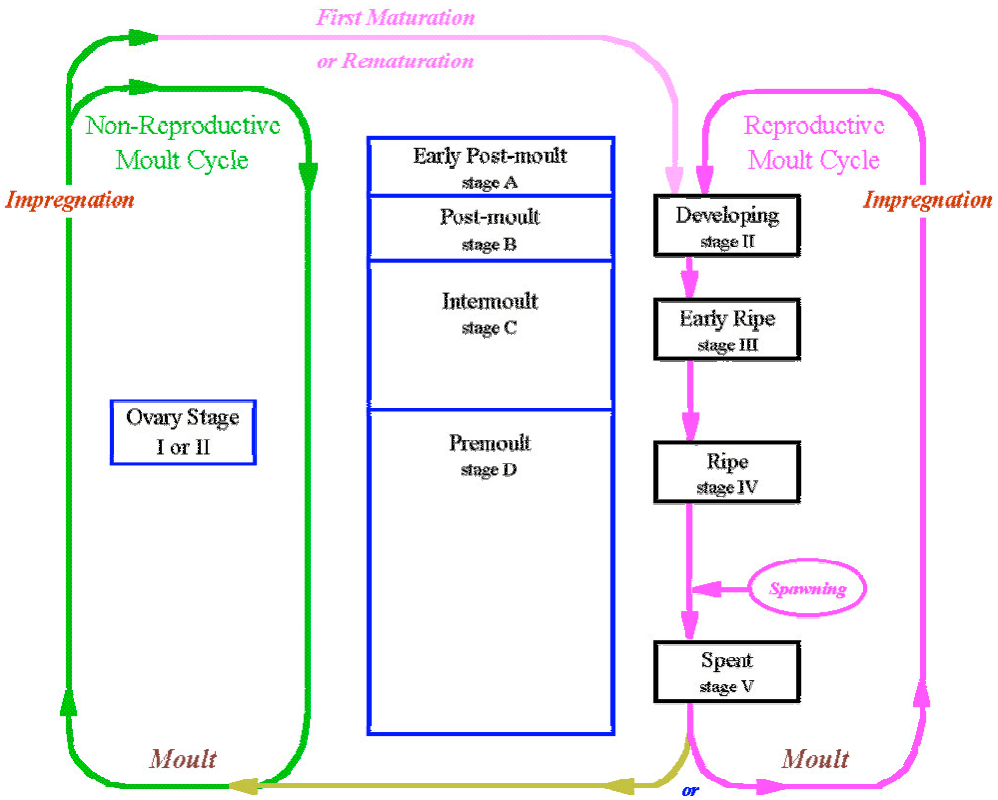

Fig. 9 Maturation, spawning and moulting of *Penaeus merguiensis* in the Gulf of Carpentaria.

1.5 Life cycle of penaeid shrimp

The penaeid life cycle includes several distinct stages that are found in a variety of habitats (shallow water to maximum 45 meters on muddy bottoms) (Fig. 10). Juveniles prefer brackish shore areas and mangrove estuaries as their natural environment. Banana shrimps can become sexually mature at about 6 months of age. Most of the adults migrate to deeper offshore areas with higher salinities, where mating and reproduction takes place. Eggs are shed into the water prior to the moult and are fertilised externally by sperm from the male. Females can lay between 100,000 to 400,000 eggs, and they can be laid in several batches (Seafood Fishing Aquaculture Marine, 2006, available: http://www.sea-ex.com/fishphotos/prawn,.htm). The eggs hatch into the first larval stage, which is the nauplius. Nauplii have limited swimming ability and usually are a part of oceanic plankton. The nauplii feed on their reserves of egg yolk, vitellin for a few days and develop into the protozoeae. The protozoeae or zoeae can feed on algae since their mouth parts and the abdomen have begun to develop, and metamorphosis into mysis. The mysis feed on algae and zooplankton, show the early development of legs and antennae, and develop into postlarva. The walking and swimming legs have now developed fully and the postlavae appear as miniature shrimp and move into the estuaries. Postlaval shrimp develop directly into juvenile shrimp which are similar to adults except they have a much longer rostrum and growth rapidly. Sub-adults move into the deeper waters or estuaries, growth rate is slower than juveniles but do not exhibit any signs of ovarian maturity yet. Adults may be 5-8 inches in length, are usually found in the ocean, mature and breed, which completes the life cycle. The maximum life span is approximately 12-18 months. To enable growth, shrimp (and all other crustaceans) periodically loosen their extracellular cuticle from the underlying epidermal layer called moulting.

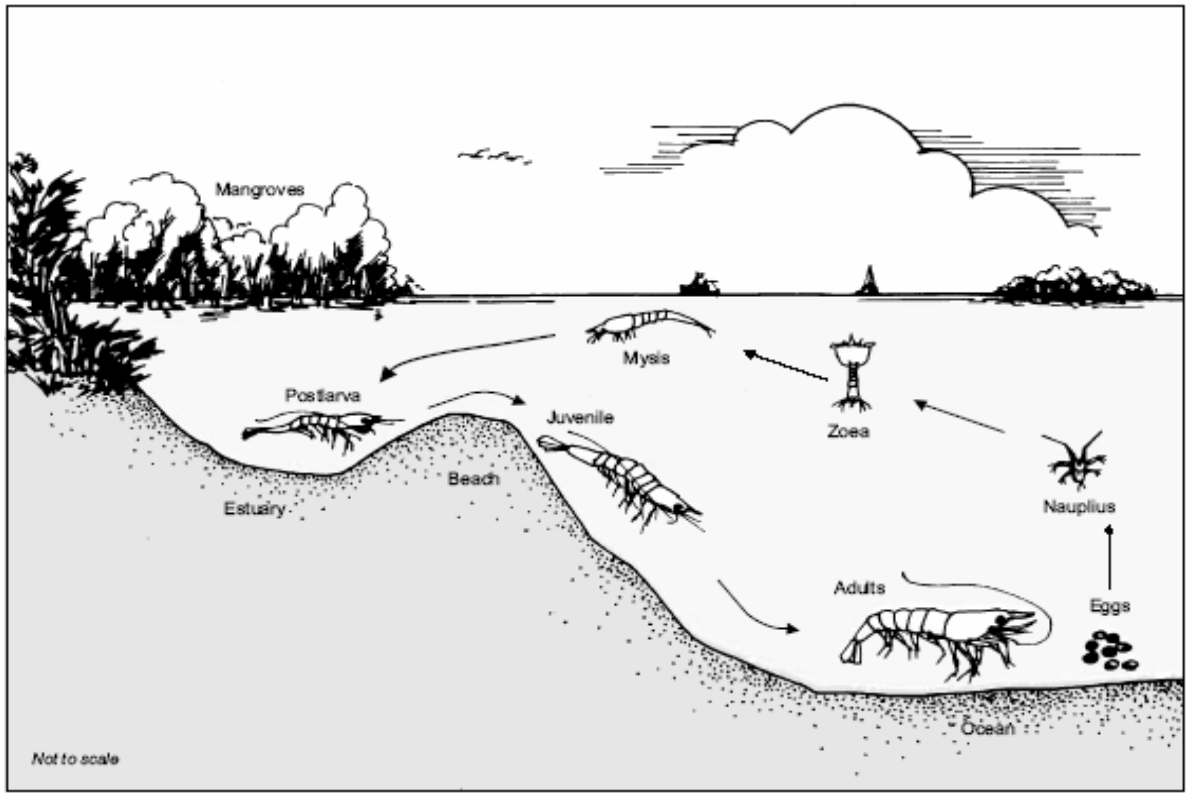

Fig. 10 The life history of penaeid shrimps.

Eggs hatch within 16 hours after fertilization. The larval stages comprise nauplius (6 stages in 2 days), protozoea/zoea (3 stages in 5 days), mysis (3 stages in 4-5 days), postlarvae and early juvenile (6-35 days). The transition from juvenile to subadult takes 135-255 days and subsequently completion of sexual maturity occurs within 10 months (Motoh, 1984). Pictures are not in proportion to actual size.

2. Vitellogenesis, vitellogenin and vitellin

Vitellogenesis is the process of biosynthesis of yolk proteins, their transport and storage in the ovary (Charniaux-Cotton, 1985). Vitellogenesis is broadly divided into two phase, Vitellogenesis I, a period of slow oocyte growth and vitellogenesis II, one of rapid ovarian growth preceding oviposition and significant increases in oocyte diameter (Meusy and Charniaux-Cotton, 1984; Meusy and Payen, 1988). The major component of yolk proteins are called lipovitellin and phosvitin in oviparous vertebrates, and vitellin (Vt) in Crustacea and other invertebrates which located in the ovary. Vitellogenin (Vg) is the precursor of Vt, which has been detected in the hemolymph of vitellogenic females in all crustacean species (Meusy, 1980; Suzuki, 1987; Quackenbush and Keeley, 1988, Shafir *et al*., 1992; Lee *et al*., 1997a; Okumura and Aida, 2000; Auttarat *et al*., 2006).

The yolk proteins are synthesized as large molecular weight proteins (300-500 kDa) that experience specific and limited cleavage into several peptide chains (Anderson *et al*., 1998). Additionally, carotenoid, sugar and lipid moieties are attached during biosynthesis (Quackenbush, 2001). Thus the yolk proteins serve as storage proteins providing amino acids, carbohydrates, lipid, phosphates and sulfates to the developing embryo (Byrne *et al*., 1989). They also store as trace mineral such as zinc (Zn^{2+}) and calcium (Ca^{2+}) (Montorzi *et al*., 1995). Canthaxanthin is the main carotenoid pigment in egg some species of anostracans (Gilchrist, 1968). In carotenoid-lipoprotein complexes, the lipid-protein interaction is reportedly stabilized by carotenoids (Cheesman *et al*., 1967). Such pigment complexes may also function as light shields protecting the embryo against harmful radiation (Adiyodi and Subramoniam, 1983).

Vg transported from its site of synthesis via hemolymph to the developing oocytes, where it is sequestered and processed into Vt, with addition of polysaccharides and lipids (Tsukimura, 2001). However, anatomical observations of the mature ovary and hepatopancreas indicate that the terminations of hepatopancreas ducts are located in left and right ovary sac, thus hepatopancreas products do not need to circulate through the hemolymp to reach the ovary, they could pass between the tissues via these ducts (Quackenbush, 2001). The internalization of Vg by the developing oocyte is accomplished via receptor-mediated endocytosis, as has been demonstrated by electron microscope and ultrastructural immunolocalization of Vg in chicken (Schneider, 1992) and invertebrates such as mosquitoes

(Sappington *et al*., 1995) and crab, *Scylla serrata* (Warrier and Subramoniam, 2002). The Vg receptor (VgR) has been found to belong to the low-density lipoprotein receptor (LDLR) super family (Bujo *et al*., 1994). In mosquito, Vg and VgR are observed together on the cell surface, in coated pits, coated vesicles and early endosomes (Snigirevskaya *et al*., 1997). However, after fusion of endosomes to produce a transitional yolk body, the Vg and VgR become separated, with VgR being recycled to the plasma membrane in tubular compartments, and Vg accumulating in the core of the transitional yolk body as shown in Fig. 11 (Sappington and Raikhel, 1998).

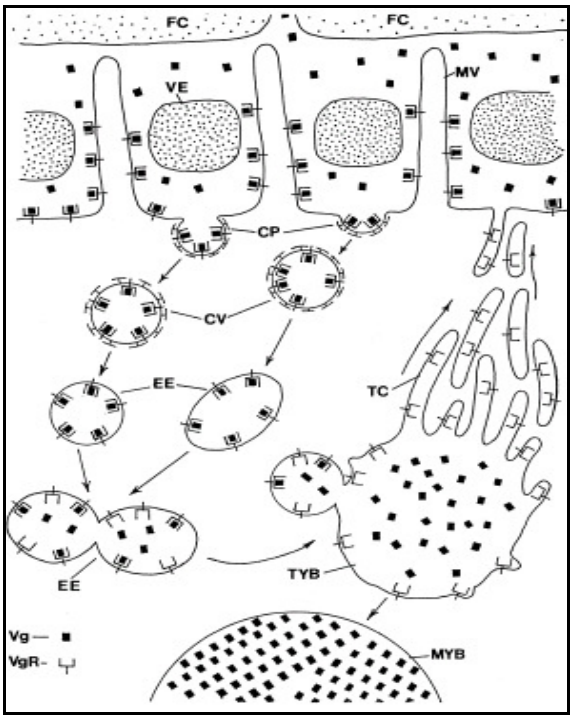

Fig. 11 Schematic interpretation of the endocytotic pathway and subsequent routing of Vg and Vg receptor (VgR) during Vg internalization by mosquito oocytes.

Vg is delivered to the oocyte in the hemolymph, entering between follicle cells (FC) and through pores of the Vt envelope (VE), and binds its receptor located in the binding microdomains of the oocyte plasma membrane. Vg/VgR complexes cluster in clathrin-coated pits (CP), which invaginate into the cytoplasm and pinch-off to form coated vesicles (CV). Upon losing their clathrin coat, the CV are transformed into early endosomes (EE) that fuse with one another to form late endosomes or transitional yolk bodies (TYB). Dissociation of Vg from its receptor probably occurs simultaneously with fusing of the early endosomes and their transformation into TYBs. In the TYB, the sorting and accumulating compartment, Vg is found free inside the vesicular reservoir, whereas VgR remains in the membrane. The recycling of VgR from the TYB to the oocyte surface occurs via the tubular compartments (TC), which are labeled for VgR but not for Vg. In contrast, Vg is delivered to the mature yolk bodies (MYB) where it is crystallized and stored until the onset of embryonic development. MV, Microvillus (Snigirevskaya *et al*., 1997).

3. Site of vitellogenin synthesis

Vg is synthesized in extraovarian tissues such as the liver in vertebrates (Byrne *et al*., 1989), fat body in insects (Raikhel and Dhadialla, 1992) and intestine in nematodes (Sharrock, 1983). In decapod crustaceans, the site of yolk protein or Vg synthesis appears to vary among crustacean species. In the past, vitellogenesis has been studied by immunological methods, immunohistochemistry and radioactive incorporation technique as shown in Table 3 (Tsukimura, 2001).

Recently, the hepatopancreas and/or ovaries were reported to be the sites of synthesis of Vg/Vt based on the expression levels of Vg mRNA, a very sensitive and acceptable measurement using Northern blot and reverse transcription-polymerase chain reaction (RT-PCR) techniques. In decapod crustaceans, the sites of Vg synthesis are ovary or hepatopancreas or both tissues depending on species and which technique was used for determination. Ovary and hepatopancreas have been reported as sites of vitellogenesis in *P. semisulcatus* (Avarre *et al*., 2003), *P. japonicus* (Tsutsui *et al*., 2000), *P. hypsinotus* (Tsutsui *et al*., 2004), *P. monodon* (Tiu *et al*., 2006), *L. vannamei* (Raviv *et al*., 2006) and *Cherax quadricarinatus* (Abdu *et al*., 2002; Serrano-Pinto *et al*., 2004) whereas in *M. rosenbergii* (Yang *et al*., 2000; Jasmani *et al*., 2004), *C. feriatus* (Mak *et al*., 2005) and *Portunus trituberculatus* (Yang *et al*., 2005) only hepatopancreas seems to be the site of Vg synthesis. These variable results may reflect the general existence of multiple sites of Vg synthesis in crustacea, or may be a result of differences in the methods used.

Table 3 Sites of decapod crustacean Vg synthesis as determined by immunological methods, immunohistochemistry or radioactive incorporation technique.

Suborder/Species	Sites of vitellogenesis	References
Dendrobranchiata:		
Litopenaeus vannamei	Hepatopancreas and ovary	Quackenbush, 1992
Marsupenaeus japonicus	Ovary	Yano and Chinzei, 1987
Penaeus semisulactus	Hepatopancreas and ovary	Browdy *et al*., 1990
		Fainzilber *et al*., 1992
		Shafir *et al*., 1992
		Khayat *et al*., 1994a
Pleocyemata:		
Callinectes sapidus	Ovary	Lee and Watson, 1995
		Lee and Walker, 1995
Carcinus maenas	Hepatopancreas	Paulus and Laufer, 1987
Homarus americanus	Hepatopancreas and ovary	Dehn *et al*., 1983
Libinia emarginata	Hepatopancreas	Paulus and Laufer, 1987
Macrobrachium lanchesteri	Hepatopancreas	Khoo *et al*., 1990
Macrobrachium rosenbergii	Hepatopancreas	Sagi *et al*., 1995
		Lee and Chang, 1997
Procambarus clarkia	Ovary	Lui *et al*., 1974
		Lui and O'Connor, 1976
Scylla serrata	Hepatopancreas	Rani and Subramonium, 1997
Uca pugilator	Ovary	Eastman-Reks and Fingerman, 1985

4. Vitellogenin processing

Vg processing and cleavage site(s) is usually determined by SDS-PAGE, N-terminal amino acid sequence, Western blotting and comparison with deduced Vg sequence. Most insect Vgs are derived from cleavage of a single precursor protein, which is recognized by subtilisin-like endoproteases at motif (R/K)-X-(R/K)-R or R-X-X-R (Barr, 1991), in the fat body and after extensive processing Vgs are secreted into the hemolymph. Vgs are probably sequestered by specific receptors on the ovarian surface and stored in the oocyte. Vertebrate Vgs are synthesized in the liver and are enzymatically processed into several subunits consisting of lipovitellins (LV1 and LV2) and phosvitins, only after internalization by the oocyte (Byrne *et al*., 1989; Retzek *et al*., 1992; Sappington and Raikhel, 1998; Polzonetti-Magni *et al*., 2004; Yoshizaki and Yonezawa, 1994). Phosvitin has a high serine content, reaching 50% in some vertebrates, and most of these serine residues are phosphorylated (Byrne *et al*., 1989). In the nematode, *Caenorhabditis elegans*, Vgs are synthesized in intestine and are neither cleaved before nor after uptake by the oocytes (Sharrock, 1983).

In the crayfish *C. quadricarinatus*, posttranslational modification by N-linked oligosaccharides and the glycosylation sites of Vg from the hemolymph were determined using a combined approach of immunoblotting, in-gel deglycosylation and mass spectrometry (Khalaila *et al*., 2004). Crustacean Vgs are enzymatically digested soon after their synthesis in the extraovarian tissues, and further cleavage takes place in the hemolymp or in the ovary (Avarre *et al*., 2003; Okuno *et al*., 2002; Mak *et al*., 2005; Tsutsui *et al*., 2000)

In *M. rosenbergii*, only one site in the Vg molecule is cleaved by subtilisin endoprotease: (R-X-R-R), (Arg707 to Arg710). This happens immediately after translation from Vg mRNA or at least before its excretion to the hemolymph. The second site of cleavage is five amino residues removed from the R-X-R-R, (Arg1742 to Arg1745) site. This cleavage takes place in the hemolymph by an enzyme of unknown identity to generate three subunits that are presumably then sequestered by the ovary (Okuno *et al*., 2002). A schematic representation of the structure of Vg and Vt, and a proposed model for vitellogenesis in penaeid species is shown in Fig. 12. A gene encoding Vg is transcribed in the hepatopancreas and ovary, and the corresponding mRNA is translated into the precursor protein, Vg. Vg first undergoes a cleavage between positions 710 and 711, just after translation of its mRNA, by subtilisin endoprotease that

must be present in both organs. At this stage, the protein is referred to as Vg. Vg from hepatopancreas is released into the hemolymp and remains in this form whereas Vg in ovary undergoes a second cleavage between position 1795 and 1796, which probably occurs with a certain delay. At this stage, there still are two possibilities: 1) the second cleavage occurs in the producing cell i.e. follicle cell (Tsutsui *et al*., 2000) and Vt is transferred to the oocytes; or 2) the second cleavage occurs in the oocytes and it is Vg that is transferred to the oocytes to be later cleaved into Vt. Whether ovarian Vg is first released into the hemolymph to later be taken up by the oocytes and then cleaved into Vt remains unknown (Avarre *et al*., 2003). In *L. vannamei* the cleavage site at position 725–728, recognized by subtilisin endoprotease (RTRR) is indeed cleaved as determined by N-terminal amino acid sequencing (Garcia-Orozco *et al*., 2002) and matrix-assisted laser desorption ionization time-of-flight (MALDI-TOF) (Raviv *et al*., 2006). In the red crab *C. feriatus*, the Vg precursor is cleaved at the RERR site (Arg714 to Arg717) and five amino acid residues downstream from a KLSR site (Lys1781 to Arg1784) (Mak *et al*., 2005).

The alignment of deduced amino acid sequences of Vg in several decapod crustacean species at the first and second cleaved sites are showed in Fig. 13 A and B, respectively (Tsutsui *et al*., 2004). Additionally, small peptides may arise from instability of the Vg precursor since in the mud crab, *S. serrata*, purified Vg possesses an intrinsic protease activity, and undergoes autoproteolysis into several small proteins (Warrier and Subramoniam, 2003). Vg from teleosts, in its purified form, is sensitive to proteolysis, which resulted in several smaller protein fragments (Hickey and Wallace, 1974; De Vlaming *et al*., 1980; Norberg and Haux, 1985; Utarabhand and Bunlipatanon, 1996).

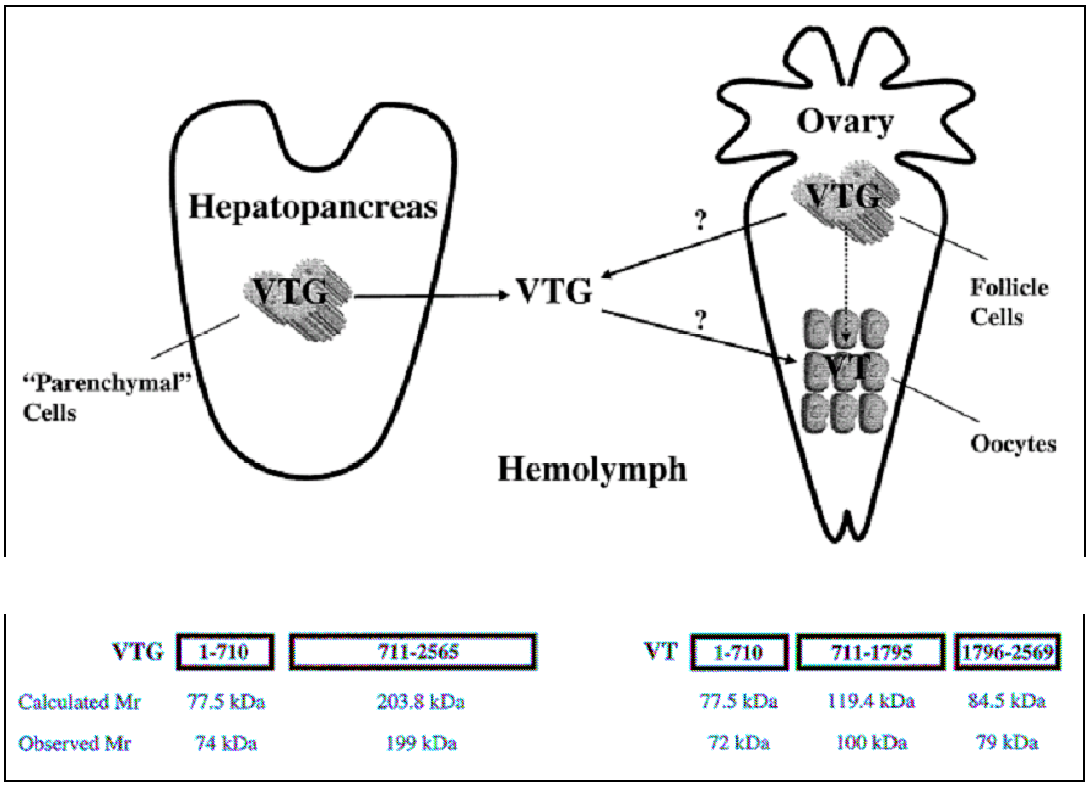

Fig. 12 Schematic representation of proposed model for vitellogenesis in penaeid species.

Vg is composed of two subunits, whereas Vt is composed of three subunits. The calculated molecular masses from the deduced amino acid sequence of the resulting subunits are shown and compared with those of the corresponding subunits observed on the Coomassie blue-stained gel. A gene encoding Vg is transcribed in the hepatopancreas and the ovary, and the Vg mRNA is translated into the precursor protein. In hepatopancreas, the precursor protein is cleaved between positions 710 and 711 to give rise to two subunits that are excreted into the hemolymph; whether hemolymph Vg (or VTG) is taken up by the oocytes and cleaved a second time is still unknown. In ovary, there are two possible pathways: 1) the precursor protein undergoes two cleavages in the follicle cells and is directly transferred to the oocytes; and 2) the precursor protein undergoes a first cleavage between positions 710 and 711 in the follicle cells and a second cleavage between positions 1795 and 1796 in the oocytes. Whether ovarian Vg is first released into the hemolymph to later be taken up by the oocytes and cleaved a second time also remains unknown (Avarre *et al.*, 2003).

Fig. 13 Partially alignment of the deduced amino acid sequence of decapod crustacean Vgs.

A, N-terminal amino acid sequence of VtB, located between subunit A and B just after cleavage site which recognized by subtilisin endoprotease (RQKR) of *P. hypsinotus*, and corresponding sequences of other Vgs. B, The N-terminal sequence context of VtC/D of *P. hypsinotus* Vg, and corresponding sequences of other Vgs. The consensus cleavage sequences for processing by endoproteases of the subtilisin family are shown in white lettering with black background in A and B. The N-terminal residue of VtC in *P. hypsinotus* and the equivalent residue in other species, where identified is surrounded by a square in B. Numbers in parentheses indicate the amino acid positions counted from the actual or putative N-terminus of each pro-Vg (Tsutsui *et al*., 2004).

5. Dynamics of Vg mRNA expression by real-time PCR

In giant freshwater prawn, *M. rosenbergii*, the dynamics of Vg mRNA expression in the hepatopancreas and ovary at different stages in both intact and eyestalk ablated females was determined by *in situ* hybridization (Jasmani *et al*., 2004) and real-time RT-PCR (reverse transcription-polymerase chain reaction) (Jayasankar *et al*., 2002). They found that Vg mRNA levels in the hepatopancreas gradually increases during moult cycle concomitant with the increasing gonadosomatic index (GSI) in intact prawns, whereas in eyestalk ablated prawns, Vg synthesis seems to be accelerated. Vg mRNA expression was negligible in the ovary of both intact and eyestalk ablated animals. The change in Vg mRNA expression in juveniles of giant freshwater prawn was examined using real-time RT-PCR, showing that in eyestalk ablated prawn, Vg mRNA expression was observed several days after ablation, Vg mRNA levels increased gradually with increasing GSI and Vg mRNA levels were negligible in the ovary, whereas in non-ablated juveniles Vg could not be detected (Jayasankar, *et al*., 2006).

In kuruma prawn, *Marsupenaeus japonicus*, the dynamics of Vg gene expression also differs between intact and eyestalk ablated animals. These were determined using real-time RT-PCR indicating that Vg mRNA levels in intact shrimps were maintained at low levels during the previtellogenic stage, and thereafter, levels in the ovary and hepatopancreas increased as vitellogenesis progressed but decreased during the later stages of maturation. In the ovary, the highest levels were observed during the early exogenous vitellogenic stage, and thereafter rapidly decreased, whereas in the hepatopancreas, high levels were maintained until the onset of the late vitellogenic stage. In contrast, in eyestalk ablated shrimp, mRNA levels differed in both tissues; an obvious increment of Vg mRNA levels were observed in the ovary whereas levels were negligible in the hepatopancreas (Tsutsui *et al*., 2000; Tsutsui *et al*., 2005).

Relative levels of Vg mRNA in the ovary and hepatopancreas in intact, induced subadult *L. vannamei* females at different times during the moult cycle were determined by real-time PCR, showing significantly higher levels of Vg mRNA in the ovary than in the hepatopancreas in endocrinologically induced females at all moult cycle stages (Raviv *et al*., 2006). Vg transcripts were also determined by real-time PCR during vitellogenesis and moult

cycle in ovary and hepatopancreas from *P. semisulcatus*. The result indicated that relative Vg mRNA levels in ovaries and hepatopancreas were significantly lower in previtellogenic (post-moult) than in vitellogenic, late vitellogenic and previtellogenic (intermoult) females. In intermoult previtellogenic females relative Vg mRNA level in ovaries was six times higher than in hepatopancreas. However, the relative levels were nearly equal between the tissues in vitellogenic and late vitellogenic female (Avarre *et al*., 2003).

6. Vg cDNA sequence and deduced amino acid comparison

The Vg gene itself encodes Vg and Vt proteins in marine shrimp (Khayat *et al*., 1994b). To date, full-length Vg cDNA have been cloned in crustacean from the following 11 species: the banana shrimp *Penaeus merguiensis* (this study), the green tiger shrimp *Penaeus semisulcatus* (Avarre *et al*., 2003), the Pacific white shrimp *Liptopenaeus vannamei* (Raviv *et al*., 2006), the black tiger shrimp *Penaeus monodon* (Tiu *et al*., 2006), the kuruma shrimp *M. japonicus* (Tsutsui *et al*., 2000), the greasy back shrimp *Metapenaeus ensis* (Kung *et al*., 2004; Tsang *et al*., 2003), the coonstriped shrimp *Pandalus hypsinotus* (Tsutsui *et al*., 2004), the giant freshwater prawn *Macrobrachium rosenbergii* (Okuno *et al*., 2002), the crayfish *Cherax quadricarinatus* (Abdu *et al*., 2002), the red crab *Charybdis feriatus* (Mak *et al*., 2005) and the japanese blue crab *Portunus trituberculatus* (Yang *et al*., 2005).

Full length Vg genes from decapod crustaceans share 50-80% sequence identity (Tiu *et al*., 2006). The Vg sequence of *L. vannamei* ORF (open reading frame) was divided into three segments along their length, and the percentage similarity of deduced Vg sequence in each segment, compared to the same segment of Vg from other decapod crustaceans are shown in Table 4 (Raviv *et al*., 2006). Although *M. ensis* is a penaeid species, it gave intermediate identity value. Among all decapod Vg sequences, the rate of amino acid substitution downstream of amino acid 1050 is higher than for the upstream region (Raviv *et al*., 2006). The most conserved region is from the N-terminal region to the conserved cleavage site around position 728 in decapods as shown in Fig. 14.

Table 4 Similarity of the three segments in *Litopenaeus vannamei* Vg sequence to all known decapod Vg sequence.

Species	% identity of the *L. vannamei* Vg sequence		
	aa 1-1050	**aa 1051-2300**	**aa 2301-2587**
P. merguiensis (This study)	89	85	87
P. semisulcatus (Avarre *et al*., 2003)	90	83	89
M. japonicus (Tsutsui *et al*., 2000)	84	73	81
Average	**88**	**80**	**86**
M. ensis (Tsang *et al*., 2003)	69	56	73
C. quadricarinatus (Abdu *et al*., 2002)	52	35	48
P. hypsinotus (Tsutsui *et al*., 2000)	51	30	47
M. rosenbergii (Okuno *et al*., 2002)	47	27	43
Average	**50**	**31**	**46**

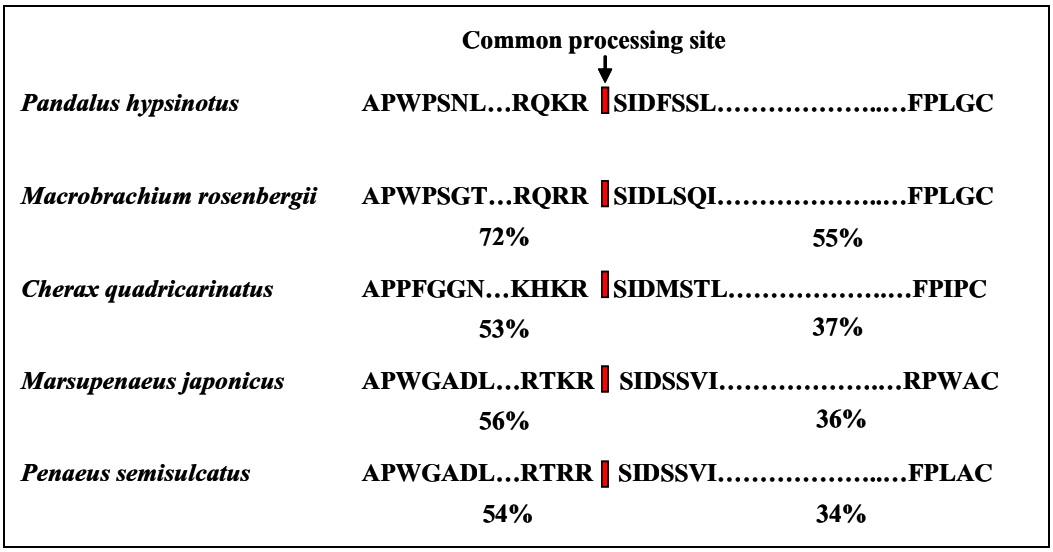

Fig. 14 Representation of Vg primary sequence in significant shrimp and prawn species.

Percentage amino acid identity is given, compared to *Pandalus hypsinotus*.

Location of a common processing site is indicated by the arrow (Wilder *et al*., 2002).

Recently, the presence of multiple genes encoding Vg in *M. ensis* (Tsang *et al*., 2003; Kung *et al*, 2004), *P. monodon* (Tiu *et al*., 2006), *C. quadricarinatus* (Serrano-Pinto *et al*., 2004) and *Daphnia magna* (Tokishita *et al*., 2006; Kato *et al*., 2004) has been reported. In the greasy back shrimp, *M. ensis*, a specific Vg gene is expressed only in a specific tissue, hepatopancreas (Tsang *et al*., 2003). Additionally, smaller transcripts specific to Vg mRNA were also detected in the hepatopancreas of *C. feriatus* (Mak *et al*., 2005; Chan *et al*., 2005) and *M. ensis* (Kung *et al*., 2004) by Northern blot analysis, suggesting that these small transcripts may be produced by post-transcriptional modification of the large transcript due to alternative splicing of the Vg gene.

In *L. vannamei*, the Vg ORF sequence does not possess any potential N-glycosylation sites. Screening all known decapod Vg sequences for basic conditions for N-glycosylation motifs (Asn-X-Ser/Thr) suggests the following: Vgs of the penaeids *M. japonicus* and *P. merguiensis* contain no potential N-glycosylation sites whereas *P. semisulcatus* and *M. ensis* contain 1, and 2 or 3 potential sites, respectively (Raviv *et al*., 2006). In sharp contrast to these dendrobranchiata species, the pleocyemata species *C. quadricarinatus*, *M. rosenbergii*, *and P. hypsinotus* contain 11, 11, and 10 potential N-glycosylation sites, respectively (Raviv *et al*., 2006). In addition, experimental studies have confirmed three of the potential N-glycosylation sites are used in *C. quadricarinatus* (Khalaila *et al*., 2004). In the Vg ORF of *L. vannamei*, only one O-glycosylation site was predicted (Raviv *et al*., 2006).

The phosvitin and polyserine domains contain tandom serine repeats that are good substrates for casein kinase II-catalyzed phosphorylation (Kuenzel *et al*., 1987; Meggio and Pinna, 1988). They are implicated in receptor binding during receptor-mediated endocytosis (Wahli, 1988) in insects, and in phosphate and metal ion (Ca^{2+} and Fe^{3+}) transport associated with bone formation in vertebrates (Wahli, 1988; Nardelli *et al*., 1987). They may also promote solubility of the Vg (Gerber-Huber *et al*., 1987). Vg in crustaceans lacks the phosvitin and polyserine domains found in many vertebrates and insects, suggesting that crustaceans may use a different mechanism for Vg-receptor binding during endocytosis of Vg molecule (Yang *et al*., 2005). A Vg-specific receptor has been found in the crab *S. serrata* (Warrier and Subramoniam, 2002).

7. Evolutionary analysis and background

Vg from invertebrates (nematode *C. elegans* and the fruit fly *D. melanogaster*) were note to be homologous with part of apolipoprotein B-100 (ApoB-100) and lipoprotein lipase from human, suggesting that copies of a precursor gene, serving a function similar to Vg, was modified to code for part of ApoB-100 and lipoprotein lipase in vertebrates (Baker, 1988). Phylogenetic reconstructions of Vgs based on sequence identities indicated that the insect lineage is the most diverged and the mammalian serum protein, ApoB-100, arose from a Vg ancestor after the nematode/vertebrate divergence (Chen *et al*., 1997). Amino acid sequence similarities are found among Vg, ApoB and apolipophorin (Apo) (Baker, 1988; Byrne *et al*., 1989; Chen *et al*., 1997; Hagedorn *et al*., 1998). Shoulders (1993 and 1994) demonstrated that microsomal triglyceride transfer protein (MTP) is homologous to the lipovitellin 1 (LV1) subunit of Vg. Babin (1999) demonstrated that Apo, ApoB-100, Vg and MTP genes are derived from a common ancestor, and also suggested that mammalian ApoB and insect Apo can be considered as paralogous to Vg. Phylogenetic analysis by Kato (2004) suggested that the large lipid transfer module or lipoprotein N-terminal domain of *D. magna* Vg1 and Vg2 are more closely related to Vg of insects than Vg of decapod crustaceans even if *D. magna* is a member of cladoceran crustaceans.

In addition, clotting protein is homologous to Vg and certain other lipoproteins such as mammalian ApoB and MTP, there share a limited sequence similarity at lipoprotein N-terminal domain and also von Willebrand factor type D domain (Hall *et al*., 1999a).

Orthologs are genes in different organisms which are direct evolutionary counterparts of each other and were inherited through speciation, as opposed to paralogs which are genes in the same organism which evolved by gene duplication. In brief, two genes are considered orthologous if their divergence is due to speciation event whereas two genes are considered paralogous if they their divergence is due to a duplication event (Fitch, 1970; Koonin, 2001). After duplication, paralogous proteins may experience different evolutionary pressures and their specificity diverges leading to emergence of new specificities and functions. Orthologous proteins, on the other hand, must be under similar regulation, have the same function and usually the same specificity in close organisms (Gelfand *et al*., 2000). So, both paralogs and

orthologs are assumed to have similar general biochemical functions, and be derived from a common ancestor, but orthologs are much closer in function.

8. Tertiary structure of lipovitellin from lamprey

The polyalanine model of the lipovitellin-phosvitin complex from silver lamprey (*Ichthyomyzon unicuspis*) oocytes was determined at a resolution of 2.8 A° (Raag *et al*., 1988). The X-ray structural studies at ambient temperature revealed several different protein domains including a large cavity in each subunit of the dimeric protein. To use the cDNA sequence for interpreting the electron-density map of lipovitellin (LV), the cleavage sites in the Vg precursor had to be determined (Sharrock *et al*., 1992). Some were obtained by N-terminal analyses of purified peptides; others were estimated by counting residues based on molecular weights obtained with SDS–PAGE (sodium dodecyl sulfate-polyacrylamide gel electrophoresis). The refined molecular structure of lipovitellin was described using synchrotron cryocrystallographic data to 1.9 A° resolution (Thompson and Banaszak, 2002). An important result from this crystallographic study at 100 K is the appearance of some bound ordered lipid along the walls of the large binding cavity. The exact identification of the lipid is difficult because of discontinuities in the electron density. The sequence of lamprey Vg was submitted in GenBank with the accession code M88749 and the structure of lamprey LV was submitted to Protein Data Bank (PDB) and its PDB ID is 1LSH. The primary sequence for the Vg precursor (Fig. 15) and how it relates to the X-ray study is shown in Fig. 16 (Anderson *et al*., 1998). In the lamprey system the larger molecular weight chain, LV1, is cleaved into two segments, hereafter referred to as LV1n and LV1c. Thus, the crystal structure is formed from three separate polypeptide chains: LV1n, LV1c and LV2. There are three predominantly antiparallel β-sheet domains, referred to as the N sheet, A sheet and C sheet, and a large helical domain. The 12 strands of the N sheet domain are formed from LV1n and include residues 17–296. Exceptions for the two β strands located within a long loop (residues 186–207). The main sheet structure is only one β strand short of closing off to form a barrel-like domain. The connection between the domain structure and the proteolytic processing of the precursor is unclear (Anderson *et al*., 1998). An extensive helical domain follows with a conformation best described as a superhelical right-handed, coiled coil with a two-helix repeating unit. The lipid cavity is covered with residues form the C-sheet and the A-sheet.

There are very few interactions between these two β-sheets domains. Side chains that line the cavity walls are mainly hydrophobic. The main lipid-binding cavity is shaped much like a funnel with two major openings to the external solvent. Ribbon diagrams of lipovitellin complete with ordered lipid are shown in Fig. 16 (Anderson *et al*., 1998) and Fig. 17 (Thompson and Banaszak, 2002).

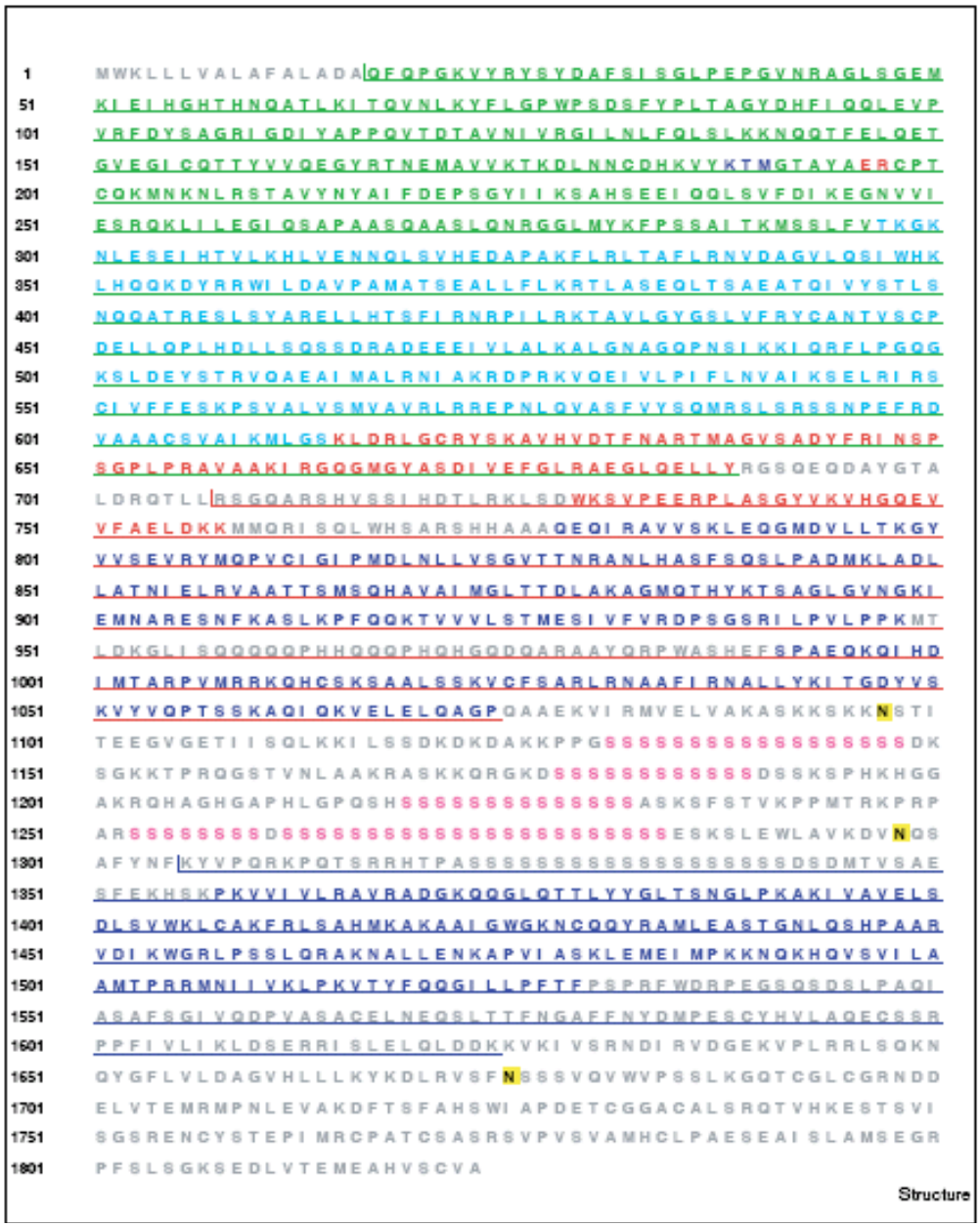

Fig. 15 Amino acid sequence of lamprey Vg and the crystal structure components.

From Fig. 15, residues not present in the X-ray model of lipovitellin (LV) are colored a medium gray unless otherwise noted, residues are indicated as being present in one of the three LV chains by colored lines below the residue. In addition, a colored bar is located to the left of the N-terminal residue of each chain. As the experimental detail definitively defining the C-terminal residue is lacked, the presumed termini are not bound by lines. Chain LV1n is indicated with green lines beginning with Gln17, and ending with Tyr688. Chain LV1c is indicated with red lines, beginning with Arg708 and with the assumed ending at Pro1074. Chain LV2 is indicated with blue lines beginning with Lys1306 and ending at Lys1624, as described in the text. In contrast to the underlining, the color of the one letter amino acid code indicates its location in the domain structure of LV as obtained from the crystallographic analysis. Colors correspond to the illustration in Fig. 16. Green characters indicate the residues that form the N-sheet domain, roughly Gln17 to Val296. Cyan characters mark those residues forming the large helical domain, Thr297 to Ser614. Red is used to denote the amino acids forming the C-sheet domain, Lys615 to Tyr688 and Trp729 to Lys758. Dark blue letters mark the residues forming the large A-sheet domain, Gln778 to Lys948, Ser991 to Pro1074 and Pro1358 to Phe1529. The three potential N-glycosylation sites (Asn1097, Asn1298 and Asn1675) are indicated with yellow boxes. Between Ser1131 and Ser1284 there are five polyserine regions (18, 12, 14, 8 and 23 amino acids long) drawn in magenta; this region is within the putative phosvitin region of lamprey LV (Anderson *et al*., 1998).

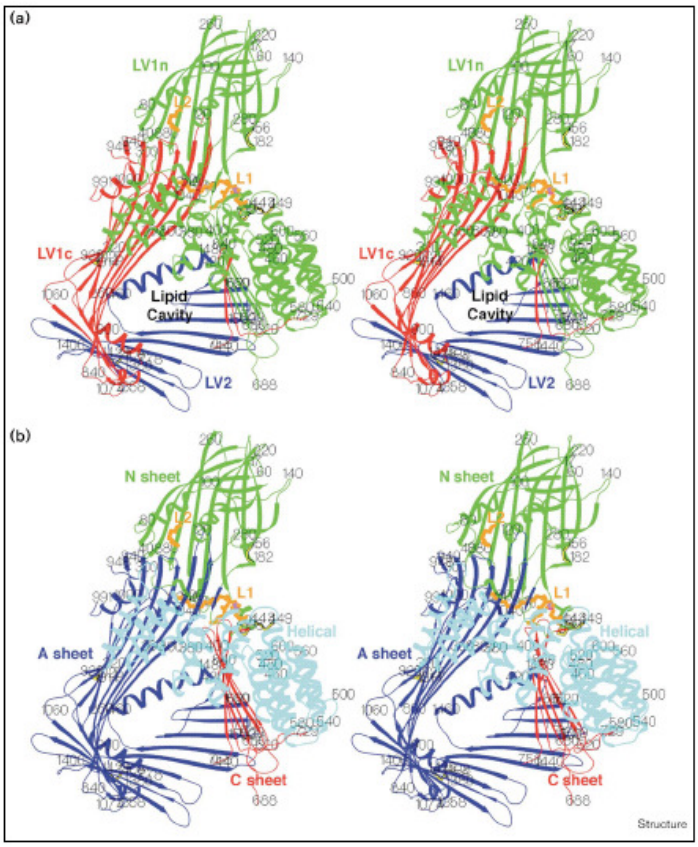

Fig. 16 Stereoview ribbon diagrams of the lamprey LV monomer.

(a) The view looking down into the funnel-shaped cavity with the widened anterior. The cartoon is color-coded to show the amino acid sequence organization in the crystal structure. Residues belonging to LV1n (Gln17 to Tyr688) are shown in green, residues belonging to LV1c (Trp729 to Lys758, Gln778 to Lys948 and Ser991 to Pro1074) are in red, and LV2 residues (Pro1358 to Phe1529) are in dark blue. The lipid ligands, L1 and L2, are drawn in orange, with the phosphate atom of L1 shown as a sphere in purple. The N and C termini of each chain are labeled with a residue number. In addition, approximately every twentieth residue is labeled. Bonds have been drawn in yellow along the C_{α}-S-S-C_{α} atom positions for the five disulfide bonds (Cys156–Cys182, Cys198–Cys201, Cys443–Cys449, Cys1014–Cys1025 and Cys1408–Cys1429). (b) The colors on the protein ribbon have been changed to illustrate the domain organization of the monomer. The structural domains are color-coded: the N-sheet domain is shown in green, the helical domain in cyan, the C-sheet domain in red, and the A-sheet domain in dark blue (Anderson *et al.*, 1998).

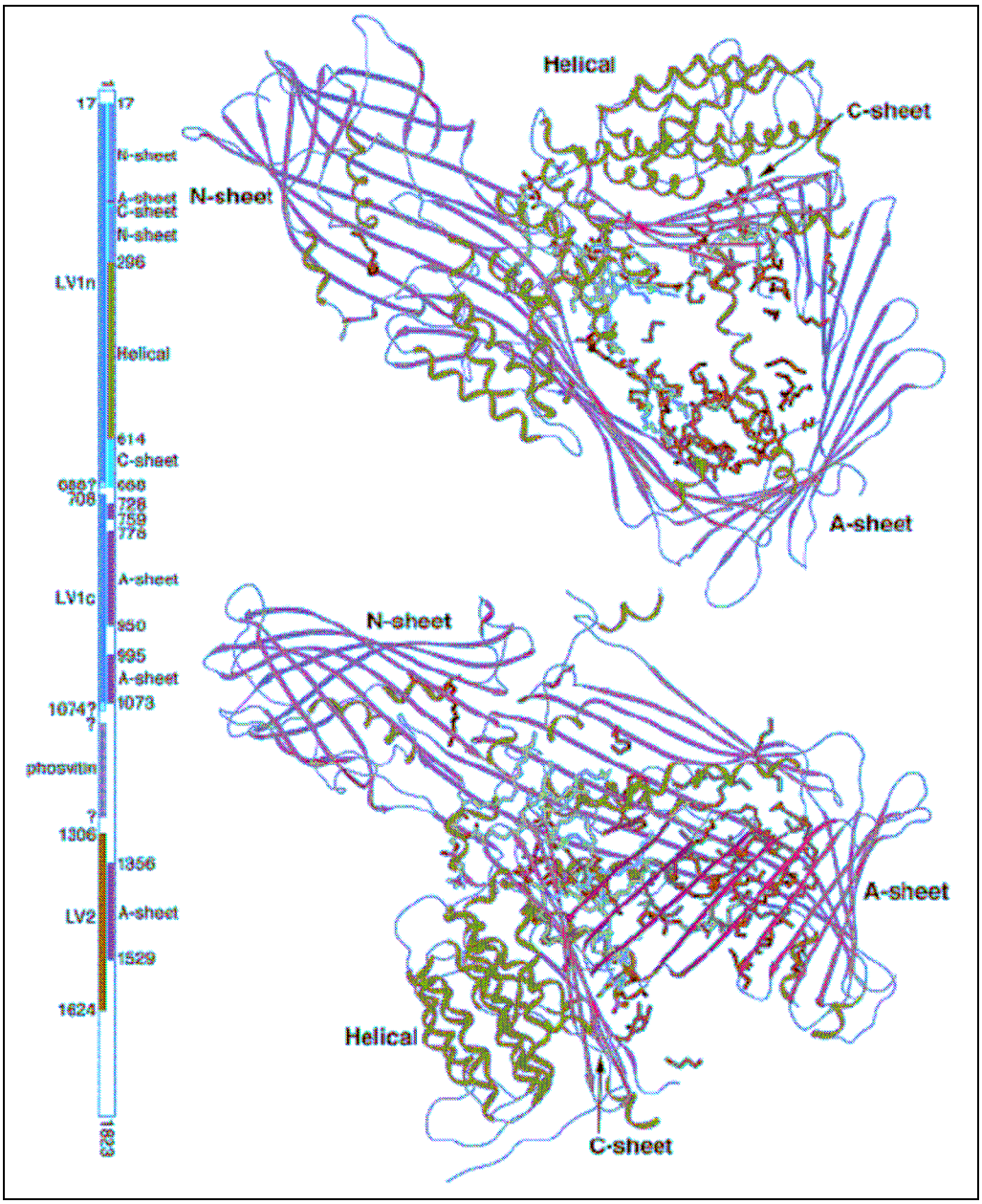

Fig. 17 Overall structure of the lamprey LV.

From Fig. 17, two views are shown of the ribbon structure of the present crystallographic model of lamprey lipovitellin (LV) with bound lipid. A color gradient from blue (background) to maroon (foreground) is used for the ribbons representing β-strands to provide depth. All R-helices are in red. The thin, yellow-orange linking segments are loops and meandering coil. The upper image was composed to best show the interior of the lipid-binding cavity at the bottom right. The lower picture was oriented to provide some perspective but also a clearer idea of the cavity shape and contents. The amino terminus of the protein is to the top left in both views beginning with the N-sheet domain and with the helical domain following. The C-sheet lines the inner side of the helical domain. Finally, an extensive A-sheet completes the polypeptide structure. The binding cavity is mainly surrounded by the inward-pointing side chains of the C- and A-sheets. The bars at the left indicate how the single polypeptide chain of Vg is proteolytically cleaved while being taken up by the ovaries. The components of this sequence visible in the electron density map are denoted by the bars to the right. In the case of lamprey, multiple segments are formed. Only LV1n, LV1c, and LV2 are visible in the model. LV1n contains the N-sheet, the helical domain, and regions of the two β-sheet structures surrounding the lipid cavity, the A- and C-sheets. The LV1c and LV2 proteolytic segments form the remainder of the C-sheet that is observed. The brown-colored model segments represent the positions of hydrocarbon chains. Finally, portions of phospholipid molecules are visible with gray-green carbon atoms (Thompson and Banaszak, 2002).

9. Genomics/EST analysis in shrimps and proteomics during early embryo development

Differences in protein expression during early embryo development have been studied in the fruit fly *D. melanogaster* (Sakoyama and Okubo, 1981; Trumbly and Jarry, 1983) and the zebrafish *Danio rerio* (Tay *et al*., 2006; Link *et al*., In press) by two-dimension gel electrophoresis procedure. Additionally, post-ovaulatory ageing and egg quality of rainbow trout coelomic fluid were determined by proteomic approach (Rime *et al*., 2004). EST (Expressed sequence tags) data based from eyestalk of the kuruma prawn *M. japonicus* (Yamano and Unuma, 2006) and EST based identification of gene expressed in branchiae of the black tiger shrimp *P. monodon* (Wuthisuthimethavee *et al*., 2005) were reported recently. Otherwise, little is known about proteomics or EST in crustacean.

10. Additional function of vitellogenin

The primary role of the yolk proteins, Vt is to provide nutrition to the developing crustacean embryos. Crustaceans rely on the yolk proteins for several days after release from the females for their nutrition. Crustaceans may have 60 to 90% of the total egg proteins as yolk protein or Vt (Quackenbush, 2001). The clear conservation of parts of the invertebrate and vertebrate Vg sequences with two mammalian proteins involved in lipid transport (ApoB-100) and metabolism (lipoprotein lipase) over a long time suggests that Vg may have other function than as food source (Baker, 1988).

In the mud crab, *S. serrata*, purified Vg possesses an intrinsic protease activity, and undergoes autoproteolytic cleaveage into several small proteins (Warrier and Subramoniam, 2003). A 50 kDa fragment of Vg possessing protease function was observed in the Pacific eel, *Anguilla japonica* (Komatsu *et al*., 1996). One of the Vg fragments had a protease function and aided in the fragmentation process of Vg into Vt in the sand crayfish, *Ibacus ciliatus* (Komatsu and Ando, 1992). Vg is also involved in defense reactions which determine in the rosy barb fish, *Puntius conchonius* possesses both antibacterial and hemagglutinating activities *in vitro*, and the male fish challenged with *Escherichia coli* synthesized Vg (Shi *et al*., 2006).

In sea urchin, Vg mRNA was detected in both female and male suggesting that Vg may serve two functions: its classical role as yolk protein precursor and an unidentified function required by adults of both sexes (Shyu *et al*., 1986). In the honeybee, *Apis mellifera*, Vg

is not only synthesized by the reproductive queen, but also by the functionally sterile workers. Vg is synthesized in large quantities by hive bees, thus an alternative use of Vg is a component of the proteinaceous royal jelly that is produced by the hive bees (Amdam *et al*., 2003).

Surprisingly, Vgs of *Daphnia magna* (crustacean) have a superoxide dismutase (SOD)-like domain at the N-terminal in front of the lipoprotein N-terminal domain thus Vg in *D. magna* may play a role in detoxification of superoxides resulting from Vg metabolism. It is noted that the SOD domain has low activity but in the eggs of *D. magna*, there are very large amounts of Vg. Alternatively, it may be important only as a transporter of Cu^{2+} since the amino acid residues that corresponded to binding site for Zn^{2+} are substituted or deleted in *Daphnia* SOD (Kato *et al*., 2004; Tokishita *et al*., 2006).

Objectives

1. To purify and characterize vitellin from the ovaries of vitellogenic *P. merguiensis*.
2. To clone and characterize *P. merguiensis* Vg cDNA.
3. To determine the synthesis sites of vitellogenin (Vg) in *P. merguiensis* by RT-PCR.
4. To determine changes in Vg mRNA expression during ovarian development by real-time PCR.
5. To analyze primary, secondary and tertiary structures of deduced Vg sequence from ovary of *P. merguiensis*.
6. To construct phylogenetic tree and comparative study the sequence of *P. merguiensis* Vg with Vgs and other proteins from several species of lipoprotein N-terminal domain and von Willebrand factor (vWF) type D domain.
7. To study protein expression during ovarian development by proteomic approach.